Ultrafast laser inscription of an integrated photonic lantern

R. R. Thomson,[1*] T. A. Birks,[2] S. G. Leon-Saval,[3] A. K. Kar,[1] and J. Bland-Hawthorn[3,4]

[1]*Scottish Universities Physics Alliance (SUPA), School of Engineering and Physical Sciences, Physics Department, David Brewster Building, Heriot Watt University, Edinburgh, EH14 4AS, Scotland*
[2]*Department of Physics, University of Bath, Claverton Down, Bath, BA2 7AY, UK*
[3]*Institute of Photonics and Optical Science, School of Physics, University of Sydney, NSW 2006, Australia*
[4]*Sydney Institute for Astronomy, School of Physics, University of Sydney, NSW 2006, Australia*
**R.R.Thomson@hw.ac.uk*

Abstract: We used ultrafast laser inscription to fabricate three-dimensional integrated optical transitions that efficiently couple light from a multimode waveguide to a two-dimensional array of single mode waveguides and back. Although the entire device has an average insertion loss of 5.7 dB at 1539 nm, only ≈0.7 dB is due to mode coupling losses. Based on an analysis which is presented in the paper, we expect that our device should convert a multimode input into an array of single modes with a loss of ≈2.0 dB, assuming the input coupling losses are zero. Such devices have applications in astrophotonics and remote sensing.

OCIS codes: (130.3120) Integrated optics devices; (140.3390) Laser materials processing.

References and links

1. J. Bland-Hawthorn and P. Kern, "Astrophotonics: a new era for astronomical instruments," Opt. Express **17**(3), 1880–1884 (2009).
2. P. Kern, E. Le Coärer, and P. Benech, "On-chip spectro-detection for fully integrated coherent beam combiners," Opt. Express **17**(3), 1976–1987 (2009).
3. J. Bland-Hawthorn, M. Englund, and G. Edvell, "New approach to atmospheric OH suppression using an aperiodic fibre Bragg grating," Opt. Express **12**(24), 5902–5909 (2004).
4. S. G. Leon-Saval, T. A. Birks, J. Bland-Hawthorn, and M. Englund, "Multimode fiber devices with single-mode performance," Opt. Lett. **30**(19), 2545–2547 (2005).
5. D. Noordegraaf, P. M. W. Skovgaard, M. D. Nielsen, and J. Bland-Hawthorn, "Efficient multi-mode to single-mode coupling in a photonic lantern," Opt. Express **17**(3), 1988–1994 (2009).
6. D. Noordegraaf, P. M. W. Skovgaard, M. D. Maack, J. Bland-Hawthorn, R. Haynes, and J. Laegsgaard, "Multi-mode to single-mode conversion in a 61 port Photonic Lantern," Opt. Express **18**(5), 4673–4678 (2010).
7. S. G. Leon-Saval, A. Argyros, and J. Bland-Hawthorn, "Photonic lanterns: a study of light propagation in multimode to single-mode converters," Opt. Express **18**(8), 8430–8439 (2010).
8. T. A. Birks, A. Diez, J. L. Cruz, S. G. Leon-Saval, and D. F. Murphy, "Fibers are looking up: optical fiber transition structures in astrophotonics," in Frontiers in Optics, OSA Technical Digest (CD) (Optical Society of America, 2010), paper FTuU1. http://www.opticsinfobase.org/abstract.cfm?URI=FiO-2010-FTuU1.
9. R. R. Thomson, G. Brown, A. K. Kar, T. A. Birks, and J. Bland-Hawthorn, "An integrated fan-out device for astrophotonics," in Frontiers in Optics, OSA Technical Digest (CD) (Optical Society of America, 2010), paper PDPA3. http://www.opticsinfobase.org/abstract.cfm?URI=FiO-2010-PDPA3.
10. N. Cvetojevic, J. S. Lawrence, S. C. Ellis, J. Bland-Hawthorn, R. Haynes, and A. Horton, "Characterization and on-sky demonstration of an integrated photonic spectrograph for astronomy," Opt. Express **17**(21), 18643–18650 (2009).
11. E. le Coarer, S. Blaize, P. Benech, I. Stefanon, A. Morand, G. Lérondel, G. Leblond, P. Kern, J. M. Fedeli, and P. Royer, "Wavelength-scale stationary-wave integrated Fourier-transform spectrometry," Nat. Photonics **1**(8), 473–478 (2007).
12. B. Martin, A. Morand, P. Benech, G. Grosa, P. Kern, L. Jocou, and E. Le Coarer, "Realization of the compact static Fourier transform spectrometer LLIFTS in glass integrated optics," Opt. Lett. **34**(15), 2291–2293 (2009).
13. J. Bland-Hawthorn, J. Lawrence, G. Robertson, S. Campbell, B. Pope, C. Betters, S. Leon-Saval, T. Birks, R. Haynes, N. Cvetojevic, and N. Jovanovic, "PIMMS: photonic integrated multimode microspectrograph," Proc. SPIE **7735**, 77350N (2010).
14. R. R. Thomson, A. K. Kar, and J. Allington-Smith, "Ultrafast laser inscription: an enabling technology for astrophotonics," Opt. Express **17**(3), 1963–1969 (2009).

#142500 - $15.00 USD Received 10 Feb 2011; revised 5 Mar 2011; accepted 5 Mar 2011; published 11 Mar 2011

15. K. M. Davis, K. Miura, N. Sugimoto, and K. Hirao, "Writing waveguides in glass with a femtosecond laser," Opt. Lett. **21**(21), 1729–1731 (1996).
16. R. R. Thomson, H. T. Bookey, N. D. Psaila, A. Fender, S. Campbell, W. N. Macpherson, J. S. Barton, D. T. Reid, and A. K. Kar, "Ultrafast-laser inscription of a three dimensional fan-out device for multicore fiber coupling applications," Opt. Express **15**(18), 11691–11697 (2007).
17. T. Pertsch, U. Peschel, F. Lederer, J. Burghoff, M. Will, S. Nolte, and A. Tünnermann, "Discrete diffraction in two-dimensional arrays of coupled waveguides in silica," Opt. Lett. **29**(5), 468–470 (2004).
18. C. Mauclair, G. Cheng, N. Huot, E. Audouard, A. Rosenfeld, I. V. Hertel, and R. Stoian, "Dynamic ultrafast laser spatial tailoring for parallel micromachining of photonic devices in transparent materials," Opt. Express **17**(5), 3531–3542 (2009).
19. M. Ams, G. D. Marshall, and M. J. Withford, "Study of the influence of femtosecond laser polarisation on direct writing of waveguides," Opt. Express **14**(26), 13158–13163 (2006).
20. A. A. Said, M. Dugan, P. Bado, Y. Bellouard, A. Scott, and J. Mabesa, "Manufacturing by laser direct-write of three-dimensional devices containing optical and microfluidic networks," Proc. SPIE **5339**, 194–204 (2004).
21. Y. Nasu, M. Kohtoku, and Y. Hibino, "Low-loss waveguides written with a femtosecond laser for flexible interconnection in a planar light-wave circuit," Opt. Lett. **30**(7), 723–725 (2005).

1. Introduction

Astrophotonics is the application of photonic principles to astronomical instrumentation [1]. The aim of this burgeoning field is to reduce the cost, size, weight and complexity of instruments while increasing their performance. Examples of astrophotonic devices developed so far include optical waveguide circuits for beam combination in long baseline interferometry [2] and complex fibre Bragg gratings for suppressing the fluorescence lines generated by the earth's atmosphere [3].

The "photonic lantern" (PL) [4–8] is a remarkable astrophotonic device that efficiently couples light between a multimode (MM) optical fibre and a set of degenerate single mode (SM) cores in several SM fibres [4–7] or a single multicore fibre (MCF) [4,7–9]. If the SM cores are arranged into a linear array [9], the PL can enable the collection of light from a telescope using a MM fibre and the low-loss reformatting of this light into a near diffraction limited input (in one axis) for a bulk optic spectrograph, minimising spectrometer size for a given resolution. Similarly it also facilitates the use of mass-producible photonic spectrographs based on Arrayed Waveguide Gratings (AWGs) [10], Stationary-Wave Integrated Fourier-Transform Spectrometry (SWIFT) [11] or Leaky Loop Integrated Fourier Transform Spectrometers (LLIFTS) [12]. Recently, for example, the PIMMS instrument concept has been proposed [13] which suggests that a single AWG can be used to process all the single modes produced at the output of a PL. This could be important in diverse field spectroscopy - a group of techniques which enable astronomers and space scientists to select regions of a telescope image for spectroscopic analysis.

Currently, PLs are made in two ways based on optical fibres. In the first [4–6], multiple SM fibres are stacked inside a low-index capillary. This fibre-filled capillary is then tapered down until the SM cores are too small to properly guide light. At this point the amalgamated claddings of the SM fibres become a single MM core, with the capillary acting as the cladding. If the taper is sufficiently gradual, it forms a low-loss adiabatic transition between this MM core and the SM fibres. A low-loss device has been made which efficiently couples the output of a MM fibre into a set of 61 SM cores and back [6]. However, this method is highly labour intensive and prohibitively expensive for mass-production. To overcome this drawback, PLs can instead be made using MCFs [8]. A single MCF with over 100 individual SM cores is placed inside the low-index capillary instead of the stacked SM fibres, and this construction is tapered down to achieve the required gradual transition. Since the MCF can be drawn in km lengths and only a few metres are required for each PL, this route is potentially low cost and suitable for mass-production.

Despite the success of these fibre tapering techniques, significant benefits of cost, size, robustness and suitability for mass-production arise if PLs could be realised using integrated optical waveguides. However, because the input to the PL is MM in both orthogonal axes, integrated PLs inherently require a three-dimensional (3D) waveguide fabrication technology.

#142500 - $15.00 USD Received 10 Feb 2011; revised 5 Mar 2011; accepted 5 Mar 2011; published 11 Mar 2011

Recently we proposed [14], and here now demonstrate, that ultrafast laser inscription can be used to fabricate integrated PLs. This 3D technique uses focused ultrashort laser pulses to locally modify the structure of a dielectric material, and hence its refractive index [15]. If this modification is appropriately controlled, it can be used to directly write, or inscribe, optical waveguides by translating the material in 3D through the laser focus. This unique capability facilitates the fabrication of 3D couplers [16] and two-dimensional arrays of coupled waveguides [17,18].

2. Integrated photonic lantern fabrication

An integrated PL was fabricated using ultrafast laser inscription to produce the structure shown conceptually in Fig. 1(a). At one end, the PL consisted of 16 SM waveguides arranged in a two-dimensional 4 × 4 array, with an inter-waveguide spacing of 50 μm. At the opposite end these waveguides were brought together in 3D to form a single MM waveguide.

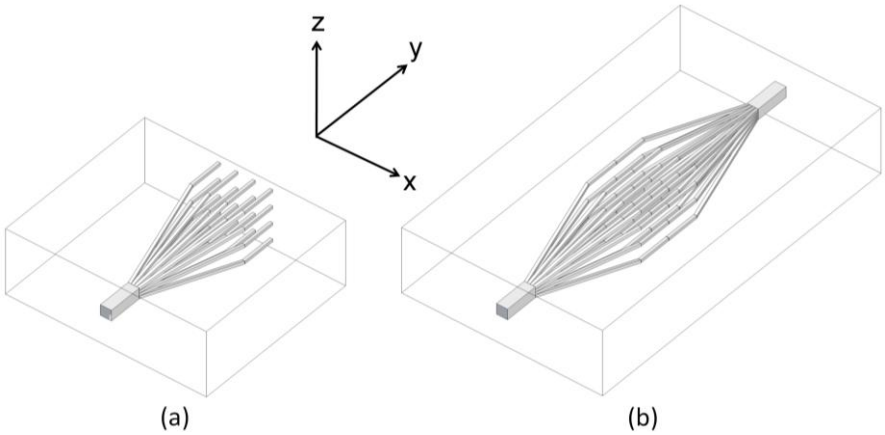

Fig. 1. Sketches of (a) a MM-to-SM integrated PL transition and (b) a MM-to-SM-to-MM transition created by inscribing two of the PLs shown in (a) back-to-back.

The substrate material was a borosilicate glass (Corning Eagle 2000) with a refractive index $n \approx 1.49$ at 1550 nm. Structures were inscribed inside the substrate using the ultrashort pulses generated by a master-oscillator power-amplifier fibre laser supplied by IMRA. The pulse energy and pulse repetition rate were set to 165 nJ and 500 kHz respectively, and the laser polarisation was set to circular. Circularly polarized light was used in order to reduce the probability of the inscribed waveguides exhibiting guiding properties which depend on the sample translation direction [19]. The measured pulse duration was ≈350 fs FWHM and the central wavelength was 1047 nm. The laser light was focused below the surface of the substrate using an aspheric lens with a numerical aperture of 0.4. To translate the sample through the focus, it was mounted on computer controlled Aerotech x-y-z air-bearing stages. All structures were inscribed using a sample translation velocity of 8.0 $mm.s^{-1}$. Throughout the paper we will consistently refer to the laser beam direction as the *z*-axis, the primary sample translation direction as the *y*-axis and the axis orthogonal to both as the *x*-axis, Fig. 1.

The induced refractive index distribution was controlled using the well established multiscan technique [20,21]. Each SM waveguide was therefore formed by scanning the sample back and forth through the laser focus 20 times (10 in each direction), with individual scans separated by 0.4 μm along *x*. The SM-to-MM transition was formed by bringing the SM waveguides together in 3D using straight waveguide paths over a *y*-axis length of 25 mm. At the end of the transition (i.e. the MM waveguide) this equates to four bands of refractive index modification, each starting and finishing at the same position along *x* but ≈8.0 μm apart along *z*. Each band was formed using 80 scans (40 in each direction) of the sample separated by 0.4

#142500 - $15.00 USD Received 10 Feb 2011; revised 5 Mar 2011; accepted 5 Mar 2011; published 11 Mar 2011

μm along *x*. The PL structures were constructed using continuous scans of the sample along its full *y*-axis length, without stopping at the interfaces between each section in the device. Thus, all sections of the device were constructed simultaneously, not individually. To avoid shadowing effects, the deepest scans were performed first and the device was built upwards layer by layer progressively towards the surface.

Three separate structures were inscribed on each of two 70 mm long substrates (substrates 1 and 2). These structures were a full MM-to-SM-to-MM transition comprising two PLs back-to-back as shown in Fig. 1(b), a matching straight MM waveguide, and a matching straight SM waveguide.

3. Photonic lantern characterization

3.1. Facet images and guided light

After inscription, substrate 1 was diced in the middle to expose the waveguide array and the exposed waveguide facets of one half were polished. We will refer to the MM, PL and SM structures on this half as MM-1, PL-1 and SM-1 respectively. Transmission mode optical micrographs of the SM array end of PL-1 and MM-1 are presented in Figs. 2(a) and 2(b) respectively.

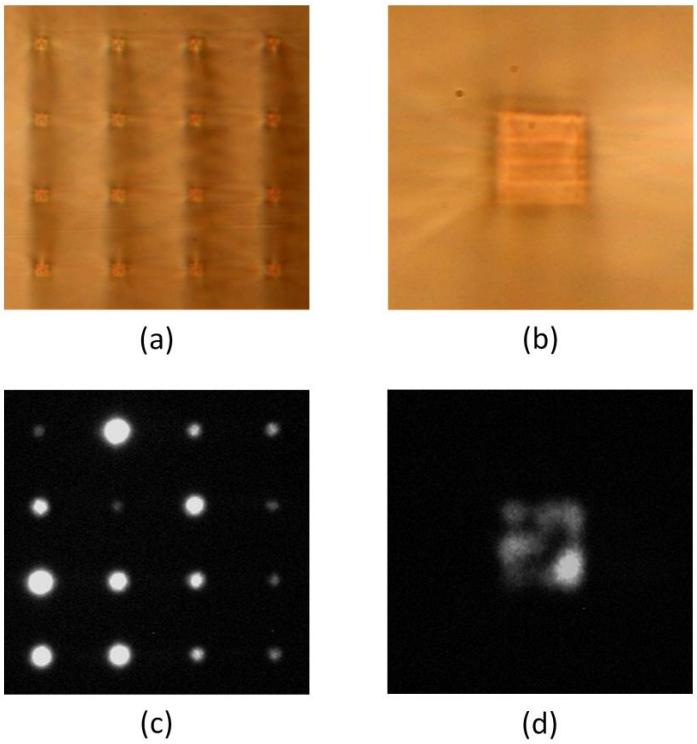

Fig. 2. White light transmission micrographs of (a) the 4 × 4 SM array end of PL-1 and (b) one end of MM-1. (c) Single frame from a near field video recording (Media 1) of the SM array end of PL-1 while adjusting the injection of 1539 nm light into the MM end. (d) Single frame from a near field video recording (Media 2) of MM-1 while adjusting the injection of 1539 nm light into the opposite end. The field of view is 200 μm × 200 μm for (a) and (c), and 100 μm × 100 μm for (b) and (d). In all cases, the inscription laser entered the sample from below.

#142500 - $15.00 USD Received 10 Feb 2011; revised 5 Mar 2011; accepted 5 Mar 2011; published 11 Mar 2011

We used 1539 nm laser light to investigate the inscribed structures. First, we coupled this light into SM-1 by direct butt-coupling from a SM fibre, while imaging the output onto a phosphor coated CCD camera. Only the TEM_{00} mode could be excited while adjusting the input coupling, indicating that the waveguide supported only a single mode. The light was then similarly coupled into the MM end of PL-1, and it was observed that the injected light did indeed couple to the SM array at the output, Fig. 2(c). Furthermore, as shown in Fig. 2(c) (Media 1), the intensity distribution across the SM array changed as the coupling was adjusted, confirming qualitatively that more than one of the modes of the MM end is coupled into the array.

The modes of MM-1 were similarly investigated, confirming that MM-1 was multimode and that the modes extended fully across the waveguide cross-section. Different transverse modes were excited as the input coupling was adjusted, Fig. 2(d) (Media 2). These observations confirm that our method of combining 16 SM waveguides into a single MM waveguide was successful.

3.2. Refractive index profile measurements

The refractive index profiles (RIPs) of MM-1 and one of the SM waveguides of PL-1 were measured by the refracted near field principle with 670 nm light using a Rinck-elektronik profiler. The measured RIP of the SM waveguide, Fig. 3, was not measured to be a well defined top-hat profile. This could be the result of convolution with the profiler point spread function (PSF), in which case it may not measure the full magnitude of the index contrast. When the profiler laser light is optimally focused onto the sample under test, we evaluated the PSF along the *z*-axis to be equivalent to a Gaussian with a FWHM size of ≈1.5 μm. We presume that the PSF along the *x*-axis is comparable. For our sample however it was non-trivial to achieve precise focusing onto the waveguide facet due to the low Fresnel reflection from the oil-glass interface (The profiler is designed to be used with silica-on-silicon waveguides where the Fresnel reflection from the silicon substrate can be used for viewing and focusing the laser). If the laser is not correctly focused onto the waveguide facet, the PSF may be significantly larger than the optimum value reported above. Regardless of these considerations, the apparent maximum index contrast of $\Delta = (n_{core} - n_{clad})/n_{core} \approx 1.76 \times 10^{-3}$ measured for the structure in Fig. 3 does at least gives an indication of the level of index change induced using the fabrication parameters described in §2.

MM-1 exhibited a high quality top-hat RIP, Fig. 4. The spatial index distribution is highly symmetric and almost 35 μm square, Fig. 4(a). However, the MM waveguide was too far below the sample surface for the profiler to measure the waveguide and the reference materials used for calibration. The profiles in Fig. 4 are therefore *normalised* and show only the uniformity and distribution of the index modification. Interestingly, from Fig. 4(b) it can be seen that the *z*-axis section through the RIP has three clear peaks where the four bands of index modification overlap. This indicates that the index modification is not fully saturated in the regions where there is no overlap between the individual bands. It should therefore be possible to further increase the refractive index contrast of the MM waveguide, either by decreasing the *x*-axis separation between adjacent scans or by reducing the sample translation speed. Lastly, it can be seen that both profiles shown in Fig. 3(a) and Fig. 4(a) appear to be slightly wider along the *z*-axis on the -*x* side of the profiles. For Fig. 4(a), this observation agrees with the optical micrograph of the structure shown in Fig. 2(b). This feature was observed to be repeatable across numerous MM structures written with these parameters. The multiscan process used to inscribe the structure shown in Fig. 3 started on the -*x* side, as did each band of modification used to fabricate the structure in Fig. 4. The narrowing of the band of modification as it is built up is therefore the result of some cumulative phenomena, the nature of which is not yet known.

#142500 - $15.00 USD Received 10 Feb 2011; revised 5 Mar 2011; accepted 5 Mar 2011; published 11 Mar 2011

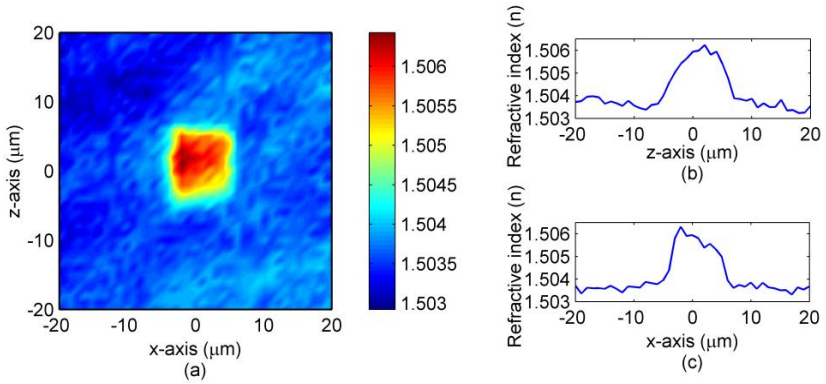

Fig. 3. (a) Two-dimensional refractive index profile of one of the SM waveguides of PL-1. The laser entered from the –z direction. (b) & (c) One-dimensional index profiles along *z* and *x* respectively, taken at $x = 0$ and $z = 0$ respectively in (a).

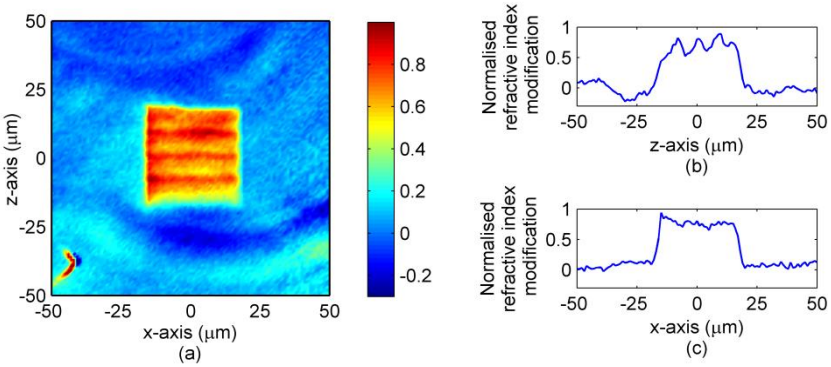

Fig. 4. (a) Two-dimensional normalised refractive index profile of MM-1 (the structure shown in Fig. 2(b)). The laser entered from the –z direction. (b) & (c) One-dimensional normalised index profiles along *z* and *x* respectively, taken at $x = 0$ and $z = 0$ respectively in (a).

3.3. Insertion loss measurements

Important considerations are the absolute loss of the integrated PL and also the coupling efficiency from the MM section into the SM array. We measured loss using MM light prepared using PL-1 as a SM-to-MM transition. 1539 nm light was coupled into each SM waveguide of PL-1 and input coupling optimized to produce different superpositions of modes at the MM end. A polarization controller after the source was used to scan all polarization states and the maximum and minimum powers at the MM end were recorded.

The MM output of PL-1 was then used as the source to characterize the losses of two structures on the 70 mm long (undiced) substrate 2: a straight MM waveguide and a full MM-to-SM-to-MM transition as shown in Fig. 1(b)). We refer to the two structures as MM-2 and PL-2 respectively (PL-2 was therefore in fact two PLs back-to-back, as shown in Fig. 1(b)). The loss was measured by directly butt-coupling the MM output of PL-1 into the structure under test and measuring the light emerging from its other end. This was repeated for light in each SM input of PL-1. We stress that the input coupling from PL-1 was not adjusted during the measurements. The average insertion loss (and polarization dependent loss) was 5.0 dB (1.1 dB) for MM-2 and 5.7 dB (1.2 dB) for PL-2. The 0.7 dB difference in average insertion loss between MM-2 and PL-2 demonstrates that mode coupling losses in the transition of PL-2 are low.

#142500 - $15.00 USD Received 10 Feb 2011; revised 5 Mar 2011; accepted 5 Mar 2011; published 11 Mar 2011

4. Discussion

The MM end of the integrated PL has dimensions of ≈35 μm × 35 μm, as expected from the inscription parameters. Although we were unable to calibrate the RIP in Fig. 4, it is reasonable to assume that the index contrast of the MM waveguide is similar to that measured for the SM waveguide in Fig. 3. Using a finite element package (Femlab), we modelled the MM end of the PL as a 35 μm square step-index waveguide with $n_{core} = 1.49263$ and $n_{cladding} = 1.49$ (i.e. $\Delta = 1.76 \times 10^{-3}$) and found 13 spatial modes (26 vector modes) at 1539 nm.

If the first (MM-to-SM) transition of PL-2 is sufficiently gradual, the 13 spatial modes of the MM input adiabatically evolve into the 13 lowest order spatial supermodes of the coupled waveguide system where the MM waveguide splits. After some distance the coupling between the SM waveguides becomes negligible and the light is contained in 16 separate degenerate SM waveguides. However, in the second (SM-to-MM) transition it is likely that all 16 supermodes would be excited as the SM waveguides reunite to form the output MM section. According to the second law of thermodynamics, only 13 of them can be efficiently coupled into the MM section and the others are radiated [4]. Assuming that all 16 supermodes are equally excited and the MM sections support only 13 spatial modes, we would expect to lose ≈20% of the light. This 0.9 dB of loss is remarkably close to the 0.7 dB difference in insertion loss between PL-2 and MM-2, suggesting that it can in future be reduced or eliminated by ensuring that each section of the lantern supports at least as many modes as the previous section.

Figure 2(c) (Media 1) illustrates that the power distribution across the SM array is sensitive to the relative phases and amplitudes of the modes of the MM entrance to the PL. However, if the transition loss for each mode is similar and the mode-number matching discussed in the previous paragraph is effective, the total throughput of the PL will remain constant regardless of the modal power and phase distribution – each section always has enough degrees of freedom to capture all the light in the previous section, however it is distributed [4]. This is an important feature of the PL for applications in astronomy where, for example, it is critical to maintain high throughput from a multimode fiber to a spectrograph, as discussed in §1. Clearly, for this application it is also necessary to match precisely the MM entrance of the PL to any input multimode fiber, to eliminate mode-dependent coupling losses between the fiber and the PL. We will investigate this in future studies.

Clearly the loss of our integrated PL is too high for some astrophotonic applications with their focus on deep space observations, but it is also clear that it should be possible to reduce the losses substantially. For example, neglecting the input and output coupling losses of MM-2 (since the MM output of PL-1 should be identical to MM-2) we estimate the attenuation of MM-2 to be ≈0.7 $dB.cm^{-1}$. Since 2.4 cm of PL-2 was straight MM waveguide performing no useful function, we have an effective insertion loss of ≈4.0 dB for the full MM-to-SM-to-MM transition (PL-2). Furthermore, many applications require only a MM-to-SM transition, so we can expect to achieve this function with 2.0 dB loss. With careful optimization of the fabrication process it should be possible to reduce these losses to the low level required for astronomy.

5. Conclusions

We have demonstrated for the first time that ultrafast laser inscription can be used to fabricate an integrated 3D optical waveguide transition that efficiently couples the modes of a multimode waveguide to a degenerate single mode waveguide array. We also demonstrated that the multiscan technique facilitates the fabrication of large cross section multimode waveguides with top-hat refractive index profiles, and that they can be constructed by spatially combining multiple single mode waveguides.

Finally, this work opens the way to a new class of monolithic instruments for astrophotonics, remote sensing and space photonics. These instruments will operate using

#142500 - $15.00 USD Received 10 Feb 2011; revised 5 Mar 2011; accepted 5 Mar 2011; published 11 Mar 2011

multimode inputs and combine functions such as dispersion, mode manipulation and detection on a single chip, removing coupling losses between components, reducing costs and increasing the instrument robustness.

Acknowledgments

This work was funded by the UK Science and Technology Facilities Council (STFC) through R. R. Thomson's Advanced Fellowship (ST/H005595/1) and by the UK Engineering and Physical Sciences Research Council (EPSRC) (Grant EP/G030227/1). T. A. Birks thanks the Leverhulme Trust for a Research Fellowship. J. Bland-Hawthorn is supported by an Australian Research Council (ARC) Federation Fellowship and S. G. Leon-Saval is supported by an ARC Australian Postdoctoral Fellowship. R. R. Thomson sincerely thanks M. Jubber of Gemfire Europe Ltd. for providing access to the refractive index profiler.

#142500 - $15.00 USD Received 10 Feb 2011; revised 5 Mar 2011; accepted 5 Mar 2011; published 11 Mar 2011